Control of Gradient-Driven Instabilities Using Shear Alfvén Beat Waves

D. W. Auerbach, T. A. Carter, S. Vincena, and P. Popovich

Department of Physics and Astronomy, University of California, Los Angeles, California 90095-1547, USA
(Received 3 May 2010; published 24 September 2010)

A new technique for manipulation and control of gradient-driven instabilities through nonlinear interaction with Alfvén waves in a laboratory plasma is presented. A narrow, field-aligned density depletion is created in the Large Plasma Device, resulting in coherent, unstable fluctuations on the periphery of the depletion. Two independent shear Alfvén waves are launched along the depletion at separate frequencies, creating a nonlinear beat-wave response at or near the frequency of the original instability. When the beat wave has sufficient amplitude, the original unstable mode is suppressed, leaving only the beat-wave response, generally at lower amplitude.

In magnetized plasmas in the laboratory, the loss of heat, particles, and momentum across the confining magnetic field is predominantly caused by turbulent transport associated with pressure-gradient-driven instabilities [1,2]. Controlling these instabilities to mitigate the transport they produce is therefore highly desirable for magnetic confinement fusion devices such as tokamaks. Direct control of gradient-driven instabilities has been achieved using arrays of electrodes or external saddle coils to induce fluctuating parallel currents in a cylindrical plasma device [3,4]. In these experiments, when the excited electric fields matched the frequency and wave number of a drift-wave mode in the device the observed turbulent spectrum collapsed onto the single coherent driven mode (synchronization) and turbulent transport is reduced [5]. Extending the transport control enabled through mode-synchronization to high-temperature fusion devices is highly desirable but it would not be possible using material electrodes. It is also not clear whether saddle coils would be effective at driving currents for synchronization in a high-performance device.

Turbulence control with core plasma access might be achieved using externally-launched radiofrequency (rf) waves. High-power rf is expected to be an important tool for heating and current drive on next-step fusion experiments such as ITER [6] and could be available for application to turbulence and transport control. Creation of flow shear for turbulence suppression [7] using rf waves has been theorized [8] and recently demonstrated in the Alcator C-Mod tokamak [9,10]. Direct modification of gradient-driven instabilities is also possible through interaction with an rf field. Control of drift-wave fluctuations was demonstrated in *Q*-machine experiments using lower hybrid waves to affect plasma properties and the drift-wave dispersion to suppress growth [11–14]. The modification of other transport related instabilities, such as the ion temperature gradient (ITG) instability, in the presence of rf driven fast magnetosonic waves has also been suggested and investigated theoretically [15].

This Letter reports on novel laboratory experiments using rf waves, in particular, shear Alfvén waves (SAWs), to modify gradient-driven instabilities. Two co-propagating SAWs with slightly differing frequency are launched along a narrow field-aligned density depletion on which coherent (dominant single-frequency) unstable fluctuations are observed. Modification and control of the instability is seen when the nonlinear beat response exceeds an amplitude threshold and the frequency of the beat wave is near the frequency of the gradient-driven instability. In this case, the original unstable mode is reduced in amplitude or suppressed completely, leaving only the beat-driven response, generally at lower amplitude. A reduction in broadband fluctuations is also observed accompanying the suppression of the primary mode. This control is observed for a finite range of beat-wave frequencies around the unstable mode frequency; this range widens with increased beat-wave amplitude.

This research was carried out on the upgraded Large Plasma Device (LAPD) at the Basic Plasma Science Facility (BAPSF) at UCLA [16]. The LAPD creates a 17.5 m long, ~0.6 m diameter cylindrical magnetized plasma lasting ≲20 ms at a repetition rate of 1 Hz. Parameters for the helium plasmas used in these experiments are $n_e \sim 10^{12}$ cm^{-3}, $T_e \sim 6$ eV, and $B = 800$ G. Measurements are made using Langmuir probes (triple probes and swept probes for plasma temperature, density, potential and fluctuations) and magnetic pick-up probes (magnetic field fluctuations). Two-dimensional average profiles are acquired over many repeatable discharges by moving a single probe shot-to-shot. Two-dimensional cross-correlation functions are achieved using a second, stationary reference probe separated axially (along the background field) from the moving probe.

Conditions are established for the instability formation through creation of a field-aligned axial density depletion embedded in the center of the LAPD plasma column. This type of condition has been extensively investigated in the LAPD, and the presence of gradient-driven

drift-Alfvén-wave instabilities in such conditions is well documented [17,18]. The depletion is formed by inserting a small metal blocking disk between the anode and cathode, selectively blocking the high energy primary electrons that ionize the neutral gas and leaving a lower temperature and density striation along the central axis of the machine. As shown in Fig. 1(a) the pressure drops by about 50% in the depletion, which is ~6 cm wide. The measurements shown are of ion saturation current ($I_{sat} \propto n_e \sqrt{T_e}$) and pressure P_e, with P_e calculated from T_e and I_{sat}. Figure 1(b) shows measured I_{sat} fluctuations, which are localized to the density gradient associated with the depletion. Figure 1(d) shows the spatially averaged fast Fourier transform (FFT) power spectrum of I_{sat}, indicating a narrow-band spectrum with power at ~6 kHz and harmonics. Cross-correlation measurements shown in Fig. 1(c) of the spontaneous fluctuations indicate a $m = -1$ azimuthal mode number for the dominant mode, with propagation in the electron diamagnetic direction. Many of the measured properties of the unstable modes (frequency, direction and speed of propagation) agree with predictions for drift waves. However, Fig. 1(e) shows that the measured phase between density fluctuations and potential fluctuations (θ_x) is approximately 180°, which is inconsistent with the $0° < \theta_x < 90°$ predictions and observations of saturated, single mode drift waves [19].

It is important to note that in these experimental conditions there are two sources of free energy, the pressure gradient and flow shear due to the variation in the profile of plasma potential. Numerical eigenmode solutions to the linearized Braginskii two-fluid equations [20] were performed, using experimentally measured density,
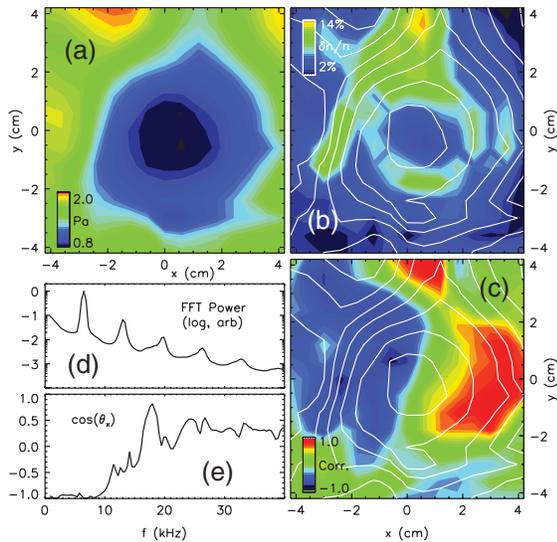
temperature, and potential profiles. These solutions indicate that drift-type and Kelvin-Helmholtz modes are linearly unstable and have real frequency approximately equal to the measured frequency, leaving open the possibility that the saturated single unstable mode observed might be of either type of instability or a hybrid mode driven by both sources of free energy.

A two-strap "picture-frame" style antenna [21,22] is inserted into the plasma at the far end of the depletion, 13 m from the plasma source. The antenna is centered on the depletion and aligned to launch SAWs along the depletion. Each strap of the antenna is driven and controlled independently, giving rise to two perpendicularly polarized, copropagating SAWs. The frequencies of the two waves are offset by a few kHz, and with each frequency near half of the ion cyclotron frequency ($f_{ci} = 304$ kHz at 800 G). The peak wave magnetic field for SAWs used in this study ranges from 0.1 to 1 G ($1 \times 10^{-4} \lesssim \delta B/B \lesssim 1 \times 10^{-3}$). In the absence of the density depletion, the two SAWs interact nonlinearly, driving a nonresonant quasi-mode at their beat frequency [23].

To investigate the interaction between the beating SAWs and the instability driven by the density depletion, a series of experiments were performed in which the beat frequency was set near the instability frequency and varied shot to shot. Figure 2(a) shows the measured I_{sat} power spectrum near the depletion gradient maximum (at approximately $x = 2$ cm, $y = -1$ cm (see Fig. 1 axes) 6 m from the antenna and 7 meters from cathode) as the beat frequency is varied over $0 \leq f_{beat} \leq 15$ kHz.

The beat-driven response is observed to be strongest when the beat frequency is close to the instability frequency (6 kHz), with peaks centered at 5.5 kHz and 8.25 kHz as shown in Fig. 2(b). In this particular data set, the peak rms amplitude of the beat response is $\delta I_{sat}/I_{sat} = 15\%$. The measured beat-wave response is significantly stronger than that observed in the absence of the depletion, where for the same launched SAW parameters, a beat-wave amplitude of $\delta I_{sat}/I_{sat} \lesssim 5\%$ is observed.

The most striking feature of Fig. 2 is the effect that the SAW beat wave has on the unstable mode at $f \sim 6$ kHz. As the beat-wave frequency approaches 6 kHz from below, the spontaneous mode begins to decrease in power and is observed to downshift in frequency, meeting the beat wave where it appears to resonate near 5.5 kHz. As the beat wave is driven to higher frequency, the spontaneous mode appears completely absent, as if the growth of the mode is suppressed in the presence of the driven response. Figure 2(b) illustrates the shift of fluctuation power from the instability to the driven fluctuations by showing the power at the unstable mode frequency (6 ± 0.4 kHz) and power in the beat-frequency band ($f_{beat} \pm 0.4$ kHz) as a function of driven beat frequency, essentially a horizontal and diagonal line cut of the data in Fig. 2(a). Also of note is the apparent reduction in broadband fluctuations while the unstable mode is suppressed. This is made clearer in Fig. 2(c), showing the measured power spectrum

FIG. 1 (color). (a) Contours of measured plasma pressure in the depletion. (b) Contours of I_{sat} fluctuation power, with pressure contours overlaid in white. (c) Cross correlation showing $m = -1$ structure of mode. (d) Spatially averaged I_{sat} FFT spectrum. (e) Spatially averaged cross-phase (θ_x) between I_{sat} and V_f fluctuations.
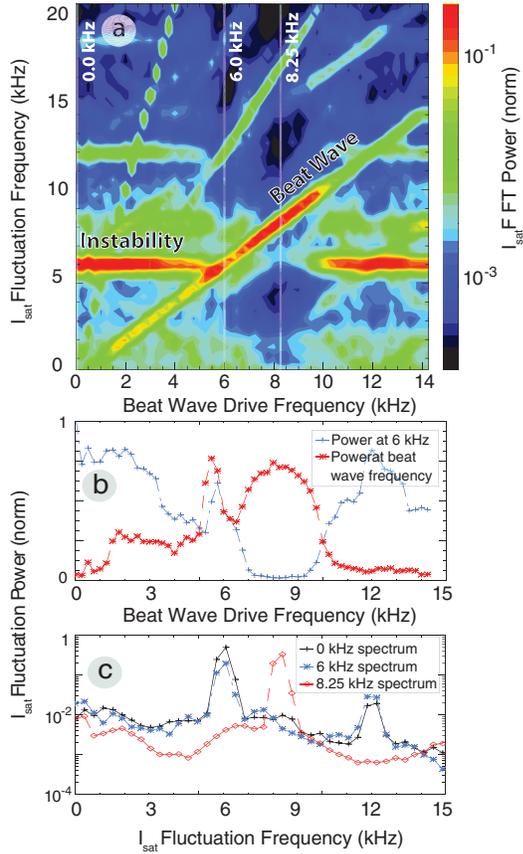
FIG. 2 (color). (Units normalized to power equivalent of maximum rms fluctuations of 15%) (a) Measured I_{sat} fluctuation power as a function of the SAW beat frequency (x axis) and FFT frequency bin (y axis). (b) Power at the spontaneous mode frequency ($f = 6 \pm 0.4$ kHz) and at the SAW beat frequency ($f = f_{beat} \pm 0.4$ kHz). (c) I_{sat} fluctuation power spectra at 0.0, 6.0, and 8.25 kHz SAW beat frequency (marked with vertical lines on the 2D bispectral plot above in part a).

in the absence of the SAW beat wave (both antennas set to the same frequency, black line), and the spectrum in the presence of a 6 kHz (blue line) and an 8.25 kHz (red line) driven beat wave. As the beat frequency is increased further, eventually the instability returns as the beat-driven response appears to diminish.

The peaks in Fig. 2(b) suggest that the SAW beat wave is resonantly driving a linear mode at $f \sim 5$ kHz and $f \sim 8$ kHz and this conjecture is supported by the spatial structure of the beat-wave response found using cross correlation measurements. Figure 3 shows the two-dimensional cross-phase (row a) and spatial distribution of fluctuation power (row b) for three cases: the spontaneous mode in the absence of SAWs (column 1), the beat-wave response when driven at 6 kHz (column 2), and the beat-wave response when driven at 8 kHz (column 3). Note that for the two beat-wave cases, the power in the beat-wave response is concentrated on the density gradient [Figs. 3(b)2 and 3(b)3], similar to the spontaneous mode [Fig. 3(b)1]. In contrast to this observation, in the absence

of the depletion, the beat wave has a much broader spatial distribution consistent with the pattern of the launched SAWs (not shown here). The correlation function of the beat-driven response at 6 kHz [Fig. 3(a)2] is nearly identical to the spontaneous mode [Fig. 3(a)1] and indicates an $m = -1$ mode structure. The beat-driven response at 6 kHz also rotates in the electron diamagnetic drift direction. The peak in the beat response at 8 kHz corresponds to an $m = -2$ mode, as shown in Fig. 3(a)3.

The appearance of the control of the instability shown in Fig. 2 depends strongly on the strength of the beat-wave drive, a parameter controlled by increasing the amplitude of the launched SAWs. Figure 4(a) shows the variation in the beat-wave and the instability amplitudes as the SAW antenna current is increased (for fixed 8 kHz beat frequency). A threshold is clear for affecting the instability, requiring the beat-wave amplitude to be on the order of 10% of the amplitude of the original unstable mode. It is also interesting to note that the beat-wave response saturates as the instability is completely suppressed. Also shown is the instability power as a function of antenna current in the case of zero beat frequency. A reduction of the instability power at high SAW amplitude is observed which can be attributed to profile modification due to electron heating by the launched SAWs [22]. This effect contributes to modification of the instability in the presence of SAWs, but is less significant than the reduction observed with nonzero beat frequency.

The width in beat frequency over which control of the instability is observed also varies with amplitude of the driven beat-wave response. Figure 4(b) shows the FFT power at the unstable mode frequency as a function of beat-wave frequency and antenna current (which controls the amplitude of the interacting Alfvén waves). At higher currents, the instability ($m = -1$) begins to be suppressed in favor of the higher frequency mode driven by the beat-wave ($m = -2$). The white contour in Fig. 4(b) indicates where the instability power is at 50% of the "background" power with the antennas driving a zero beat-frequency Alfvén-wave. The broadening of the range over which
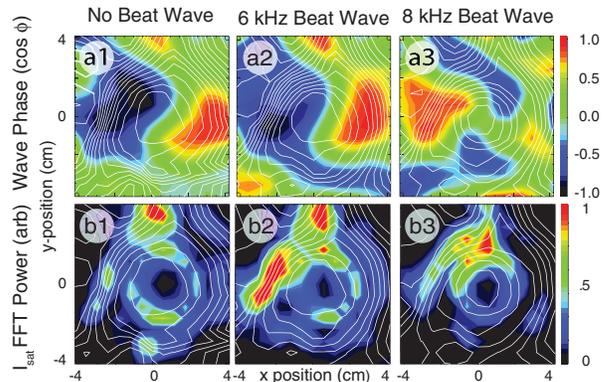
FIG. 3 (color). 2D phase (from cross correlation) and spatial power distribution of I_{sat} fluctuations for the spontaneous mode (no SAWs) and 6 and 8 kHz beat waves.
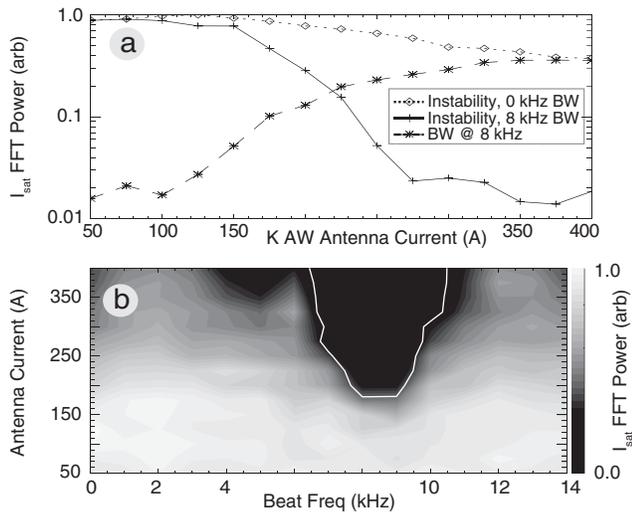
FIG. 4. (a) Power in the instability band (6.5 ± 0.4 kHz, solid line) and driven beat-response band (8.0 ± 0.4 kHz, dashed line) versus SAW drive current for the case of 8.0 kHz beat frequency, along with a reference instability power (6.5 ± 0.4 kHz, dotted line) at zero beat frequency (both antennas at same frequency). (b) Fluctuation power in the instability band (6.5 ± 0.4 kHz) vs beat-frequency vs antenna current. The white contour is the 50% suppressed level at each power.

the instability is controlled as the beat-wave power is increased is indicated by this contour. Similar observations are made in VINETA [24], where the effect was compared to "Arnold Tongues" seen in nonlinearly driven unstable oscillators [25,26].

The exact mechanism by which the beating SAWs couple nonlinearly to and control the unstable mode is still under investigation. Experiments have established that the parallel wavelength of the beat wave is essential. Beat waves generated by copropagating SAWs have very long parallel wavelength, as long or longer than the length of LAPD at low frequency [23], similar to expectations for the parallel wave number of instabilities in the depletion. Experiments were performed in which counter-propagating SAWs interacted along the depletion, driving beat waves with much shorter parallel wavelength. In this case, much smaller response at the beat frequency is observed and the control behavior shown in Fig. 4 is not achieved.

An important question is whether or not transport is affected through this beat-wave control process. The unmodified instability has density-potential cross phase [Fig. 1(e)] that is inconsistent with fluctuation-driven particle transport. Past experiments on filamentary pressure striations with dominant coherent modes in LAPD have revealed classical transport levels [27]. In the presence of the beat-wave in the experiments reported here, the density-potential cross phase is unaltered. Future experiments will investigate the interaction between SAW beat waves and broadband turbulence in LAPD, to see whether

or not transport control can be affected, as has been seen in mode-synchronization experiments on the VINETA device [5].

In summary, a novel approach to control of gradient-driven instabilities in magnetized laboratory plasmas has been presented. Beating SAWs have been observed to nonlinearly interact with and control unstable fluctuations on a filamentary density depletion in LAPD. These results provide motivation for studying the interaction between rf and instabilities in other magnetized plasmas, including fusion plasmas, e.g., ICRF beat-wave interaction with microturbulence. ICRF beat waves have been successfully used to produce measurable plasma response at the beat frequency and to excite Alfvén eigenmodes in JET and ASDEX Upgrade [28,29], motivating future experiments in which the beat-wave frequency is lowered into the range of drift-wave turbulence.

[1] W. Horton, Rev. Mod. Phys. **71**, 735 (1999).
[2] G. Tynan et al., Plasma Phys. Controlled Fusion **51**, 113001 (2009).
[3] C. Schröder et al., Phys. Rev. Lett. **86**, 5711 (2001).
[4] C. Schröder et al., Phys. Plasmas **11**, 4249 (2004).
[5] C. Brandt et al., J. Nucl. Mater. **390–391**, 380 (2009).
[6] M. Shimada et al., Nucl. Fusion **47**, S1 (2007).
[7] P. Terry, Rev. Mod. Phys. **72**, 109 (2000).
[8] J. Myra and D. D'Ippolito, Phys. Plasmas **9**, 3867 (2002).
[9] A. Ince-Cushman et al., Phys. Rev. Lett. **102**, 035002 (2009).
[10] Y. Lin et al., Phys. Plasmas **16**, 056102 (2009).
[11] N. Wolf et al., Phys. Rev. Lett. **45**, 799 (1980).
[12] K. Wong and P. Bellan, Phys. Fluids **21**, 841 (1978).
[13] R. Gore, J. Grun, and H. Lashinsky, Phys. Rev. Lett. **40**, 1140 (1978).
[14] C. Liu and V. Tripathi, Phys. Fluids **23**, 345 (1980).
[15] S. Chiu et al., Plasma Phys. Controlled Fusion **31**, 1095 (1989).
[16] W. Gekelman et al., Rev. Sci. Instrum. **62**, 2875 (1991).
[17] J. Maggs et al., Phys. Plasmas **4**, 1881 (1997).
[18] J. Penano et al., Phys. Plasmas **7**, 144 (2000).
[19] H. W. Hendel et al., Phys. Fluids **11**, 2426 (1968).
[20] P. Popovich et al., arXiv:1004.4674.
[21] Y. Zhang et al., Phys. Plasmas **15**, 012103 (2008).
[22] T. A. Carter et al., AIP Conf. Proc. **932**, 38 (2007).
[23] T. A. Carter et al., Phys. Rev. Lett. **96**, 155001 (2006).
[24] C. Brandt et al., Phys. Plasmas **17**, 032304 (2010).
[25] M. E. Koepke and D. M. Hartley, Phys. Rev. A **44**, 6877 (1991).
[26] H. G. Schuster, Deterministic Chaos (VCH, Weinheim, 1989), p. 158.
[27] A. T. Burke, J. E. Maggs, and G. J. Morales, Phys. Rev. Lett. **81**, 3659 (1998).
[28] A. Fasoli et al., Nucl. Fusion **36**, 258 (1996).
[29] K. Sassenberg et al., Nucl. Fusion **50**, 052003 (2010).